*Gazi University Journal of Science*
*GU J Sci*
*26(3):427-437 (2013)*

# Prediction of Deformation Mode of Bi-Metallic Rod Extrusion through Arbitrarily Curved Dies

Heshmatollah HAGHIGHAT[1,♠], Golam Reza ASGARI[2]

[1]*Mechanical Engineering Department, Razi University, Kermanshah, Iran*
[2]*Payam Higher Education Institute, Golpayegan, Iran*

*Received:17.05.2011 Revised:04.05.2012Accepted:15.08.2012*

**ABSTRACT**

The modes of deformation of bi-metal rods during forward extrusion through arbitrarily curved dies are studied in this paper. An analytical solution is developed to predict the mode of deformation by using the upper bound method. The effects of the yield stress ratio, shape and length of the die, extrusion ratio and frictional shear factors at the interface and the die surface are considered in the analysis. It is found that frictional shear factor at the interface, the ratio of flow stresses and die length are important parameters that can change mode of deformation from uniform deformation to cladding-type. Shape of the die, reduction in area and frictional shear factor at the die surface have not effect on the mode of deformation, although the effects are great on the extrusion pressure. The extrusion process is also simulated by using the finite element code, ABAQUS. The theoretical results show good agreement with the FEM results.

**Keywords**: Bi-metallic rod; Extrusion; Deformation mode, FEM

## 1. INTRODUCTION

During the bi-metallic rod extrusion process, owing to the differences between mechanical properties with respect to the constituent materials, bi-metallic rodsf requently exhibit a non-homogeneous deformation in the extrusion process. In general, if one constituent material is harder than the other, it will resist deformation; undergo a smaller reduction in area. It is necessary to know the conditions under which uniform extrusion or cladding may be carried out.A considerable amount of investigations has been done by different researches on the process of bi-metallic rod and tube extrusion process. Osakada et al. Described the hydrostatic extrusion of composite rods with hard cores by the upper bound method [1]. Ahmed studied the extrusion of copper clad aluminum wire [2]. Avitzur summarized the factors that affect simultaneous flow of layers in extrusion of a bimetal rod through conical dies [3]. Some of these factors include percentage reduction in area, semi-die angle, friction factor between sleeve and die wall, and ratio of core to sleeve radii. Tokuno and Ikeda verified thedeformation in extrusion of composite rods by experimental and upper bound methods [4]. Yang et al. Studied the axisymmetric extrusion of composite rods through curved dies by experimental and upper bound methods [5]. Sliwa described the plastic zones in the forward extrusion of metal composites by experimental and upper bound methods [6]. Chitkara and Aleem theoretically studied the mechanics of extrusion of axisymmetric bi-metallic tubes from solid circular billets using fixed mandrel with application of generalized upper bound and slab method analyses [7, 8]. They investigated the effect of different parameters such as extrusion ratio, frictional conditions, and shape of the dies and that of the mandrels on the extrusion pressures. Hwang and Hwang studied the plastic deformation behavior within a conical die during composite rod extrusion by experimental and upper bound methods [9]. Kazanowski et al. Discussed the influence of initial bi-material billet geometry on the final product dimensions [10]. Theflat face die was used for all experiments and proposed bi-material billet design modifications were

♠Corresponding author, e-mail:hhaghighat@razi.ac.ir

evaluated experimentally and by finite element modeling. Nowotynska and Smykla studiedtheinfluence of die geometric parameters on plastic flow of layer composites during extrusion process by experimental method [11]. Khosravifard and Ebrahimi [12] analyzed the extrusion of Al/Cu bimetal rod through conical dies by FEM and studied effect of extrusion parameters in creation of interfacial bonds.

In this paper, a method of predicting the mode of deformation in bi-metallic rod extrusion through dies of any shape by using the upper bound method is proposed. FEM simulation on the extrusion of a bi-metallic rod composed of an aluminum sleeve layer and a copper core layer is also conducted. The effects of a set of independent process parameters, including the yield stress ratio, thefractional cross-sectional area of the core, extrusion ratio, die shape and length and frictional shear factors at the interface and the die surface are investigated.

## 2. DEFORMATION MODELS

Fig. 1 is a schematic diagram of the bi-metallic rod extrusion through a die of arbitrary curved shape. The billet considered for analysis is a bi-metallic rod in which the inside material, core, is harder than the outside material, sleeve. An initially billet, made up of a rod and an annular tube of two different ductile materials with the mean flow stresses, $\sigma_c$ and $\sigma_s$, respectively, is considered. The subscripts $c$ and $s$ denote core and sleeve, respectively. The initial outer and inner radii of the combined billet are $R_{1i}$ and $R_{2i}$, respectively. The outer radius of the extruded bi-metallic rod is $R_{1f}$ and the interface radius of the final extruded rod is $R_{2f}$.

Three types of deformation modes are considered as:
(a) Both materials deform to the same reduction. This mode is called uniform deformation.
(b) The harder material remains undeformed while the softer material deforms to cover the harder material. This mode will be called cladding.
(c) The materials deform to different extrusion ratios. This mode will be called general deformation.

### 2.1. Uniform deformation

In the first considered case, core and sleeve materials deform with the same extrusion ratio. This mode of deformation is shown in Fig. 1. In zones I, II, V and VI the materials are rigid, and both materials are plastically deformed in zones III and IV. A spherical coordinate system $(r,\theta,\phi)$ is used to describe the position of the four surfaces of velocity discontinuity, $S_1 - S_4$, as well as the velocity in zones I-VI. The position of the coordinate system origin $O$ is defined by the intersection of a line, that goes through the point where the die profile starts and the outlet of the die, with the axis of symmetry.
The die surface, which is labeled as $\psi(r)$ in Fig. 1, is given in the spherical coordinate system. The interface between the core and the sleeve materials is defined by $\psi_i(r)$ which is the angular position of the interface surface as a function of the radial distance from the origin $O$.

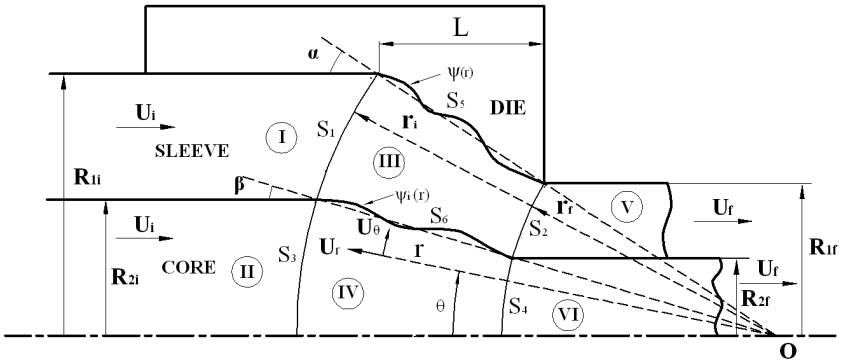


Figure 1. Kinematically admissible velocity field for uniform deformation.

### 2.2. Cladding

The other extreme mode of deformation is that when deformation occurs only in thesofter material. This is the case when hard material is cladded with a soft materialby extrusion. The inner harder material remains undeformed ( $R_{2i} = R_{2f}$ ) and it acts like a mandrel attached to the punch and moves with the punch velocity $U_i$. This mode of deformation is similar to mono-metal tube extrusion through a curved die using a moving cylindrical shaped mandrel. The considered deformation zones and velocity field for this deformation mode is shown in Fig. 2. This field can not be applied when the radius of the core material, $R_{2i}$ is

greater than the die exit radius $R_{1f}$. The zones 1 and 2 are rigid, and the sleeve material, deforms in zone 2.

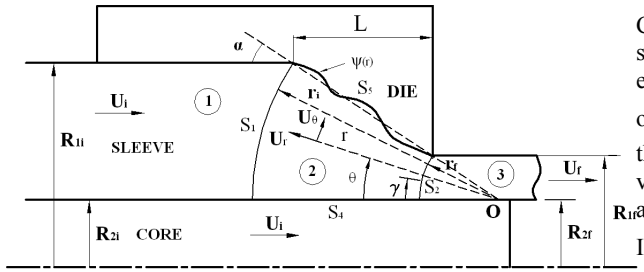


Figure 2. Kinematically admissible velocity field for cladding-type deformation.

A spherical coordinate system $(r,\theta,\phi)$ is used to describe the position of the two spherical surfaces of velocity discontinuity, $S_1$ and $S_2$, as well as the velocity in zones 1, 2 and 3. The position of the coordinate system origin $O$ is defined by the intersection of a line that goes through the point where the die profile starts and the outlet of the die, with core surface. The surface $S_1$ and $S_2$ are located at distances $r_i$ and $r_f$ from the origin $O$, respectively. The mathematical equations for radial positions of two velocity discontinuity surfaces $S_1$ and $S_2$ are given by

$$r_i = \frac{R_{1i} - R_{2i}}{\sin\alpha},\ r_f = \frac{R_{1f} - R_{2i}}{\sin\alpha} \qquad (1)$$

where $\alpha$ is the angle of the line connecting the initial point of the curved die to the final point of the die with axis of symmetry and $\tan\alpha = (R_{1i} - R_{1f})/L$, where $L$ denotes the die length.

### 2.3. The general case

Consider the general case shown in Fig. 3, where the sleeve and core materials areextruded with different extrusion ratios. Two spherical coordinate systems with origins $O_1$ and $O_2$, are used to describe the position of the four surfaces of velocity discontinuity as well as the velocities in deformation zones. The center of the entry and exit spherical boundaries of the deformation zone III, $S_1$ and $S_2$, is $O_1$ and the center of the entry and exit spherical boundaries of the deformation zone IV, $S_3$ and $S_4$, is $O_2$.

The surfaces $S_1$ and $S_2$ are located at distances $r_{1i}$ and $r_{1f}$ from the origin $O_1$, respectively and the surfaces $S_3$ and $S_4$ are located at distances $r_{2i}$ and $r_{2f}$ from the origin $O_2$, respectively. The mathematical equations for radial positions of two velocity discontinuity surfaces $S_1$ and $S_2$ are given by

$$r_{1i} = \frac{R_{1i} - x}{\sin\alpha},\ r_{1f} = \frac{R_{1f} - x}{\sin\alpha} \qquad (2)$$

where $x$ is distance of origin $O_1$ from the axis of symmetry and the mathematical equations for radial positions of two velocity discontinuity surfaces $S_3$ and $S_4$ are given by

$$r_{2i} = \frac{R_{2i}}{\sin\beta},\ r_{2f} = \frac{R_{2f}}{\sin\beta} \qquad (3)$$

where angle $\beta$, shown in Fig. 3, is given by

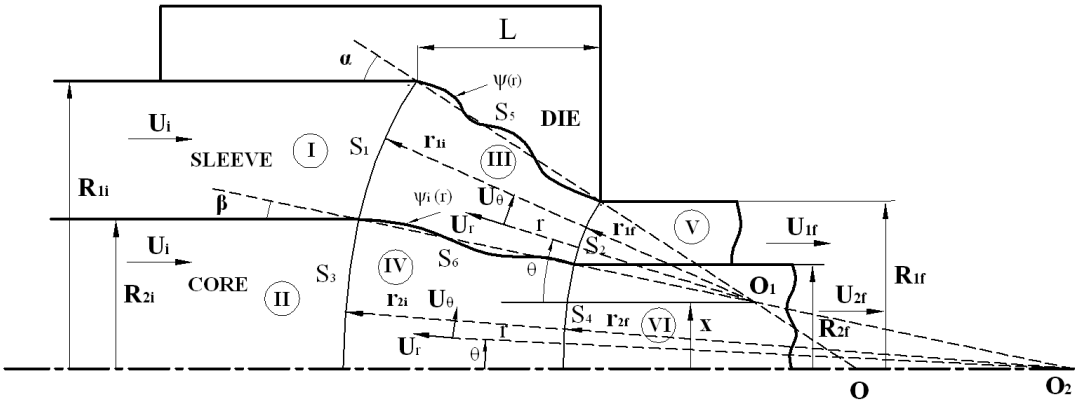


Figure 3. Kinematically admissible velocity field for the general case.

$$\sin\beta = \frac{R_{2i} - x}{R_{1i} - x}\sin\alpha \qquad (4)$$

The core material flows as if it is flowing through a curved die having an equation

$\psi_{2i}(r)$, which is the angular position of the interface surface as a function of the radial distance from the

origin $O_2$, and the radius of the inner material changes from $R_{2i}$ to $R_{2f}$.

It is clear that this field includes both uniform deformation when $x = 0$ and cladding when $x = R_{2i}$.

## 3. UPPER BOUND ANALYSIS

Based on the upper bound theory, for a rigid-plastic Von-Misses material and amongst all the kinematically admissible velocity fields, the actual one that minimizes the power required for material deformation is expressed as

$$J^* = \frac{2}{\sqrt{3}}\sigma_0 \int_V \sqrt{\frac{1}{2}\dot{\varepsilon}_{ij}\dot{\varepsilon}_{ij}}\,dV + \frac{\sigma_0}{\sqrt{3}}\int_{S_v}|\Delta v|dS + m\frac{\sigma_0}{\sqrt{3}}\int_{S_f}|\Delta v|dS - \int_{S_t} T_i v_i dS \quad (5)$$

where $\sigma_0$ is the mean flow stress of the material, $\dot{\varepsilon}_{ij}$ the strain rate tensor, $m$ the constant friction factor, $V$ the volume of plastic deformation zone, $S_v$ and $S_f$ the area of velocity discontinuity and frictional surfaces respectively, $S_t$ the area where the tractions may occur, $\Delta v$ the amount of velocity discontinuity on the frictional and discontinuity surfaces and $v_i$ and $T_i$ are the velocity and tractions applied on $S_t$, respectively.

To analyze the process in the general case, the material under deformation is divided into six zones, as shown in Fig. 3. Zones III and IV are the deformation regions that are surrounded by four velocity discontinuity surfaces $S_1, S_2, S_3, S_4$ and die surface. In addition to these surfaces, there are two frictional surfaces between die wall and sleeve, $S_5$ and interface surface between sleeve and core, $S_6$.

Assuming volume flow balance, the radial velocity $U_r$ within the deformation zone III can be obtained. In Fig. 3, the volume flow of the material across the surface $S_2$ at the point $(r_{1f}, \gamma, \phi)$ in the radial direction is

$$dQ = -U_{1f}\cos\gamma(r_{1f}d\gamma)(x + r_{1f}\sin\gamma)d\phi \quad (6)$$

where angle $\gamma$ is the angular position for point leaving deformation zone III and $U_{1f}$ is determined by

$$U_{1f} = \frac{R_{1i}^2 - R_{2i}^2}{R_{1f}^2 - R_{2f}^2}U_i \quad (7)$$

The volume flow of the material in the radial direction at the point $(r, \theta, \phi)$ in the deformation zone III is

$$dQ = U_r(rd\theta)(x + r\sin\theta)d\phi \quad (8)$$

where angle $\theta$ is angular position of a point in the deformation zone III. Equating Eqs. (6) and (8), the radial velocity component in zone III is found to be

$$U_r = -U_{1f}\left(\frac{x + r_{1f}\sin\theta}{x + r\sin\theta}\right)^2 \frac{\sin\gamma}{\sin\theta}\cos\gamma\frac{d\gamma}{d\theta} \quad (9)$$

For small distance $x$

$$\frac{x + r_{1f}\sin\gamma}{x + r\sin\theta} \cong \frac{r_{1f}}{r}\frac{\sin\gamma}{\sin\theta} \quad (10)$$

Assuming the proportional distances in a cylindrical sense from the core surface, then

$$\frac{\sin\gamma}{\sin\alpha} = \frac{\sin\theta}{\sin\psi} \quad (11)$$

where $\psi$ is the angular position of the die surface at radial distance $r$ from the origin $O_1$. Differentiating Eq. (11) yields

$$\cos\gamma\frac{d\gamma}{d\theta} = \sin\alpha\frac{\cos\theta}{\sin\psi} \quad (12)$$

Substituting Eqs. (10)-(12) into Eq. (9),the radial velocity component is simplified as

$$U_r \cong -U_{1f}\left(\frac{r_{1f}}{r}\right)^2 \frac{\sin^2\alpha}{\sin^2\psi}\cos\theta \quad (13)$$

The full velocity field for the flow of the material in zone III is obtained by invoking volume constancy. Volume constancy in spherical coordinates is defined as

$$\dot{\varepsilon}_{rr} + \dot{\varepsilon}_{\theta\theta} + \dot{\varepsilon}_{\phi\phi} = 0 \quad (14)$$

With the assumption of no rotational motion in the deformation zone (i.e. $U_\phi = 0$), the angular component of velocity field is given by

$$U_\theta \cong -U_{1f}\frac{r_{1f}^2}{r}\frac{\partial\psi}{\partial r}\left(\frac{\sin\alpha}{\sin\psi}\right)^2\frac{\sin\theta}{\tan\psi} \quad (15)$$

For deformation zone IV, the velocity field developed by Gordon et al. [13] for mono-metal rod extrusion through a die of equation $\psi_{2i}(r)$, is used as

$$U_r = -U_{2f}\left(\frac{r_{2f}}{r}\right)^2\frac{\sin^2\beta}{\sin^2\psi_{2i}}\cos\theta$$

$$U_\theta = -U_{2f}\frac{r_{2f}^2}{r}\frac{\partial\psi_{2i}}{\partial r}\left(\frac{\sin\beta}{\sin\psi_{2i}}\right)^2\frac{\sin\theta}{\tan\psi_{2i}}$$

$$U_\phi = 0 \quad (16)$$

Based on the established velocity field, the strain rate fields for zones III and IV can be obtained by

$$\dot{\varepsilon}_{rr} = \frac{\partial U_r}{\partial r}$$

$$\dot{\varepsilon}_{\theta\theta}=\frac{1}{r}\frac{\partial U_\theta}{\partial\theta}+\frac{U_r}{r}$$

$$\dot{\varepsilon}_{\phi\phi}=\frac{1}{r\sin\theta}\frac{\partial U_\phi}{\partial\phi}+\frac{U_r}{r}+\frac{U_\theta}{r}\cot\theta$$

$$\dot{\varepsilon}_{r\theta}=\frac{1}{2}\left(\frac{\partial U_\theta}{\partial r}-\frac{U_\theta}{r}+\frac{1}{r}\frac{\partial U_r}{\partial\theta}\right)$$

$$\dot{\varepsilon}_{\phi r}=\frac{1}{2}\left(\frac{\partial U_\phi}{\partial r}-\frac{U_\phi}{r}+\frac{1}{r\sin\theta}\frac{\partial U_r}{\partial\phi}\right)$$

$$\dot{\varepsilon}_{\theta\phi}=\frac{1}{2}\left(\frac{1}{r\sin\theta}\frac{\partial U_\theta}{\partial\phi}+\frac{1}{r}\frac{\partial U_\phi}{\partial\theta}-\frac{\cot\theta}{r}U_\phi\right) \quad (17)$$

With the strain rate field and the velocity field, the standard upper bound method can beimplemented. This upper bound method involves calculating the internal power of deformation over the deformation zone volume, calculating the shear power losses over the velocity discontinuity surfaces and the frictional power losses along frictional surfaces.

### 3.1. Internal power of deformation

The internal power of deformation is given by

$$\dot{W}_i=\frac{2}{\sqrt{3}}\sigma_0\int_V\sqrt{\frac{1}{2}\dot{\varepsilon}_{ij}\dot{\varepsilon}_{ij}}\,dV \quad (18)$$

where $\sigma_0$ is the mean flow stress of the material and $dV$ is a differential volume in the deformation zone. Internal power of zones I, II and V, VI are zero and the general equation to calculate the internal power of deformation in zone III is calculated as

$$\dot{W}_{iIII}=2\pi\frac{2\sigma_S}{\sqrt{3}}\int_{\eta_f}^{\eta_i}\int_{\psi_{1i}(r)}^{\psi(r)}\sqrt{\frac{1}{2}\dot{\varepsilon}_{rr}^2+\frac{1}{2}\dot{\varepsilon}_{\theta\theta}^2+\frac{1}{2}\dot{\varepsilon}_{\phi\phi}^2+\dot{\varepsilon}_{r\theta}^2}\;(x+r\sin\theta)r\,d\theta dr \quad (19)$$

where $\psi_{1i}(r)$ is the angular position of the interface surface as a function of the radial distance from the origin $O_1$ and it is assumed that

$$\psi_{1i}(r)=\sin^{-1}\left[\frac{\sin\beta}{\sin\alpha}\sin\psi(r)\right] \quad (20)$$

The general equation to calculate the internal power of deformation in zone IV is determined as

$$\dot{W}_{iIV}=2\pi\frac{2\sigma_C}{\sqrt{3}}\int_{r_{2f}}^{r_{2i}}\int_0^{\psi_{2i}(r)}\sqrt{\frac{1}{2}\dot{\varepsilon}_{rr}^2+\frac{1}{2}\dot{\varepsilon}_{\theta\theta}^2+\frac{1}{2}\dot{\varepsilon}_{\phi\phi}^2+\dot{\varepsilon}_{r\theta}^2}\;(r\sin\theta)r\,d\theta dr \quad (21)$$

where $\sigma_C$ is the mean flow stress of core material and

$$\psi_{2i}(r)=\psi_{1i}(r-\frac{x}{\sin\alpha})=\sin^{-1}\left[\frac{\sin\beta}{\sin\alpha}\sin\psi(r-\frac{x}{\sin\alpha})\right] \quad (22)$$

### 3.2. Shear power dissipation

The general equation for the power losses along a shear surface of velocity discontinuity in an upper bound model is

$$\dot{W}_S=\frac{\sigma_0}{\sqrt{3}}\int_{S_v}|\Delta v|\,dS \quad (23)$$

For velocity discontinuity surface $S_1$ :

$$\Delta v_{S_1}=U_i\sin\theta+\frac{U_i r_{1i}\left.\frac{\partial\psi}{\partial r}\right|_{r=\eta_i}\sin\theta}{\tan\alpha} \quad (24)$$

$$dS_1=2\pi(x+r_{1i}\sin\theta)r_{1i}\,d\theta \quad (25)$$

For velocity discontinuity surface $S_2$ :

$$\Delta v_{S_2}=U_{1f}\sin\theta+\frac{U_f r_{1f}\left.\frac{\partial\psi}{\partial r}\right|_{r=\eta_f}\sin\theta}{\tan\alpha} \quad (26)$$

$$dS_2=2\pi(x+r_{1f}\sin\theta)r_{1f}\,d\theta \quad (27)$$

For velocity discontinuity surface $S_3$ :

$$\Delta v_{S_3}=U_i\sin\theta+\frac{U_i r_{2i}\left.\frac{\partial\psi_{2i}}{\partial r}\right|_{r=r_{2i}}\sin\theta}{\tan\beta} \quad (28)$$

$$dS_3=2\pi r_{2i}^2\sin\theta\,d\theta \quad (29)$$

For velocity discontinuity surface $S_4$ :

$$\Delta v_{S_4}=U_{2f}\sin\theta+\frac{U_{2f}r_{2f}\left.\frac{\partial\psi_{2i}}{\partial r}\right|_{r=r_{2f}}\sin\theta}{\tan\beta} \quad (30)$$

$$dS_4=2\pi r_{2f}^2\sin\theta\,d\theta \quad (31)$$

The power dissipated on the velocity discontinuity surfaces $S_1$, $S_2$, $S_3$ and $S_4$ are determined as

$$\dot{W}_{S_1}=2\pi\frac{\sigma_S}{\sqrt{3}}\int_\beta^\alpha|\Delta v_{S_1}|\,r_{1i}(x+r_{1i}\sin\theta)\,d\theta \quad (32)$$

$$\dot{W}_{S_2}=2\pi\frac{\sigma_S}{\sqrt{3}}\int_\beta^\alpha|\Delta v_{S_2}|\,r_{1f}(x+r_{1f}\sin\theta)\,d\theta \quad (33)$$

$$\dot{W}_{S_3}=2\pi\frac{\sigma_C r_{2i}^2}{\sqrt{3}}\int_0^\beta|\Delta v_{S_3}|\sin\theta\,d\theta \quad (34)$$

$$\dot{W}_{S_4}=2\pi\frac{\sigma_C r_{2f}^2}{\sqrt{3}}\int_0^\beta|\Delta v_{S_4}|\sin\theta\,d\theta \quad (35)$$

### 3.3. Frictional power dissipation

The general equation for the frictional power losses along a surface with a constant friction factor $m$ is

$$\dot{W}_f=m\frac{\sigma_0}{\sqrt{3}}\int_{S_f}|\Delta v|\,dS \quad (36)$$

For frictional surface $S_5$ :

$$|\Delta v_5|=|U_r\cos\eta+U_\theta\sin\eta|_{\theta=\psi} \quad (37)$$

where

$$\cos\eta=\frac{1}{\sqrt{1+(r\frac{\partial\psi}{\partial r})^2}},\quad \sin\eta=\frac{r\frac{\partial\psi}{\partial r}}{\sqrt{1+(r\frac{\partial\psi}{\partial r})^2}} \quad (38)$$

and

$$dS_5=2\pi(x+r\sin\psi)\sqrt{1+(r\frac{\partial\psi}{\partial r})^2}\,dr \quad (39)$$

The power dissipated on the die surface $S_5$ can be determined as

$$\dot{W}_{f5}=2\pi\frac{m_1\sigma_S}{\sqrt{3}}\int_{\eta_f}^{\eta_i}|\Delta v_5|r\sin\psi\;dr \quad (40)$$

For frictional surface $S_6$ :

$$|\Delta v_6| = \left|(U_{rIII} - U_{rIV})\cos\eta_i + (U_{\theta III} - U_{\theta IV})\sin\eta_i\right|_{\theta=\beta} \quad (41)$$

where $\eta_i$ is local angle of the interface surface with respect to the local radial velocity component and

$$\cos\eta_i = \frac{1}{\sqrt{1+(r\frac{\partial\psi_{2i}}{\partial r})^2}}, \quad \sin\eta = \frac{r\frac{\partial\psi_{2i}}{\partial r}}{\sqrt{1+(r\frac{\partial\psi_{2i}}{\partial r})^2}} \quad (42)$$

and

$$dS_6 = 2\pi r\sin\psi_{2i}\sqrt{1+(r\frac{\partial\psi_{2i}}{\partial r})^2}\,dr \quad (43)$$

The power dissipated on the interface surface can be determined as

$$\dot{W}_{f6} = 2\pi\frac{m_2\sigma_S}{\sqrt{3}}\int_{r_{2f}}^{r_{2i}}|\Delta v_6|r\sin\psi_{2i}\,dr \quad (44)$$

The total upper bound solution for extrusion pressure is

$$P = \frac{\dot{W}_{iIII} + \dot{W}_{iIV} + \dot{W}_{s1} + \dot{W}_{s2} + \dot{W}_{s3} + \dot{W}_{s4} + \dot{W}_{f5} + \dot{W}_{f6}}{\pi U_i R_{1i}^2} \quad (45)$$

## 4. RESULTS AND DISCUSSIONS

A MATLAB program has been implemented for the previously derived equations andthe relative extrusion pressure is calculated for a series of deformation modes and a field giving the lowest extrusion pressure is found. In this calculation, the value of $x$ is varied as a parameter representing the deformation mode, where $x$ is limited between 0 and $R_{2i}$. Minimization of the total extrusion force determines the value of parameter $x$.

The developed upper bound model can be used for prediction of the mode of deformation of bi-metallic rod extrusion process through dies of any shape if the die profile is expressed as equation $\psi(r)$. Two types of die shapes were examined in the present investigation. The first die shape is conical die. The second die shape is from the work by Yang and Han [14]. They created a streamlined die shape as a fourth-order polynomial whose slope is parallel to the axis at both entrance and exit. Die shape of Yang and Han was expressed in spherical coordinate system by Ref. [15].

Figs. 4a-4b show examples of the relationship between $\frac{P}{\sigma_C}$ and $\frac{x}{R_{2i}}$ for conical and Yang and Han die shape, respectively, where $x = 0$ represents uniform deformation and $x = R_{12}$ represents cladding. The assumed extrusion conditions are the same for both conical and curved dies and they are as $R_{1i} = 15$ mm, $R_{2i} = 9$ mm reduction in area $\frac{R_{1i}^2 - R_{1f}^2}{R_{1i}^2} = 0.3$, the die length 9 mm, the frictional shear factor on the die surface $m_1$ is 0.2 and the frictional shear factor $m_2$ at the interface is 0.9. Curves are plotted for various ratios of the flow stress. As shown in Figs 4a-4b, the $\frac{P}{\sigma_C}$ versus $\frac{x}{R_{2i}}$ curves are convex upwards and the minimum value of the extrusion pressure is obtained either at $x = 0$ or $x = R_{2i}$ for both conical and curved dies. Figs 4a-4b also show that uniform deformation occurs at low extrusion ratios and die shape has not effect on the mode of deformation although the effect is great on the extrusion pressure.

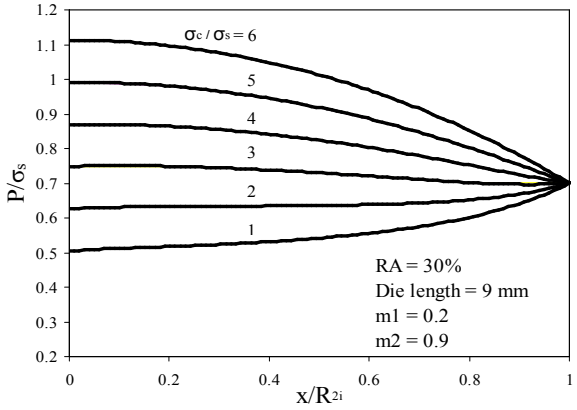


(a) Conical die

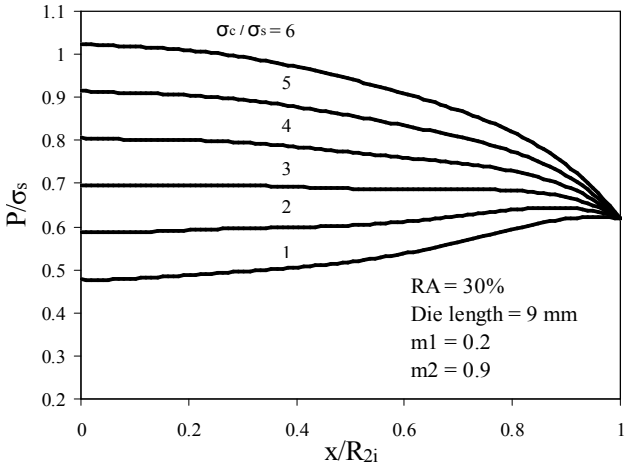


(b) Yang and Han die shape

Figure 4. Relationship between relative extrusion pressure and $\frac{x}{R_{2i}}$ for various ratios of flow stress: (a) for conical die, (b) for Yang and Han die shape.

The extrusion process is simulated by using the finite element code, ABAQUS. Considering the symmetry in geometry, two-dimensional axisymmetric models are used for FEM analyses. In each case, the whole model is meshed with CAX4R elements. Fig. 5a illustrates the mesh used to analyze the deformation in extrusion of bi-metallic rod for Yang and Han die shape and the extrusion conditions $R_{1i} = 15$ mm, $R_{2i} = 9$ mm reduction in area 0.3, the die length 9 mm, the $m_1$ = 0.2 and $m_2$ 0.9. Fig. 5b shows uniform deformation for yield stress ration 2 and Fig. 5c shows cladding mode for yield stress ration 4. By comparing the analytical results with the FEM results, it is seen that there is a good agreement between the analytical predictions and the FEM simulations.

Fig. 6 shows the effect of the friction factor between the sleeve material and the die surface $m_1$ on the mode of deformation. As shown in this figure, the effect of friction on the mode of deformation is not marked, although the effect is great on the extrusion pressure.

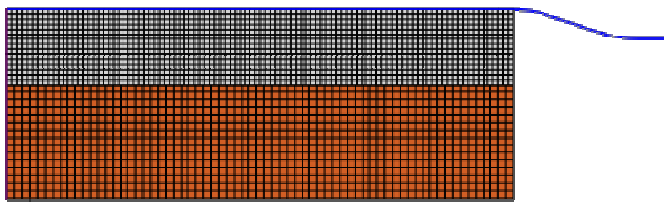

(a) The finite element mesh

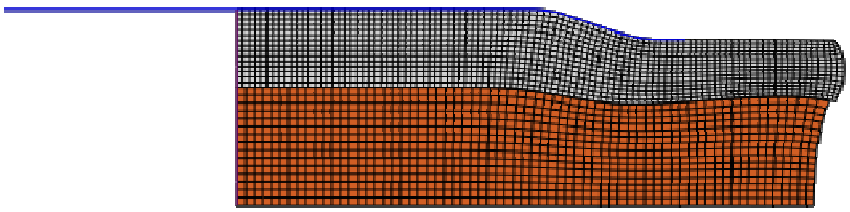

(b) The deformed mesh in uniform mode

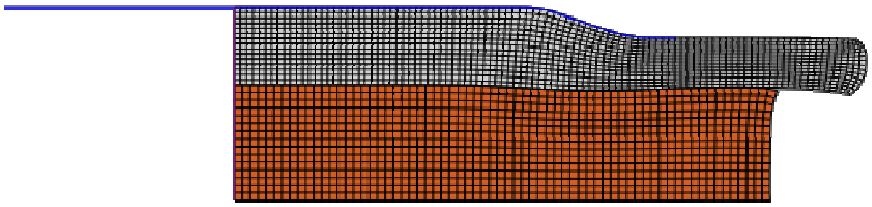

(c) The deformed mesh in cladding mode

Figure 5. (a) The finite element mesh, (b) the uniform deformation yield stress ration 2 and (c) cladding mode for yield stress ration 4( $R_{1i} = 15$ mm, $R_{2i} = 9$ mm, reduction in area 0.3 $L = 9$ mm, $m_1 = 0.2$ and $m_2 = 0.9$)

The effect of the friction factor between sleeve and core $m_2$ on the mode of deformation is also examined and it is shown in Fig. 7. It is clear that the effect of friction at the interface is one of the decisive factors, which can changes deformation mode from uniform deformation to cladding mode. When the friction at the interface is low, the deformation mode is uniform, as the frictional stress increases, the deformation mode changes to the cladding type. Uniform deformation occurs only when $m_2$ is large and the ratio of flow stresses is low. Preformed rod whose interface is bonded by adhesion tins a large value of $m_2$ and will not allow relative slip at the interface in the deformation zone. For such a preformed bi-metal rod, the main feature of the deformation mode is uniform deformation.

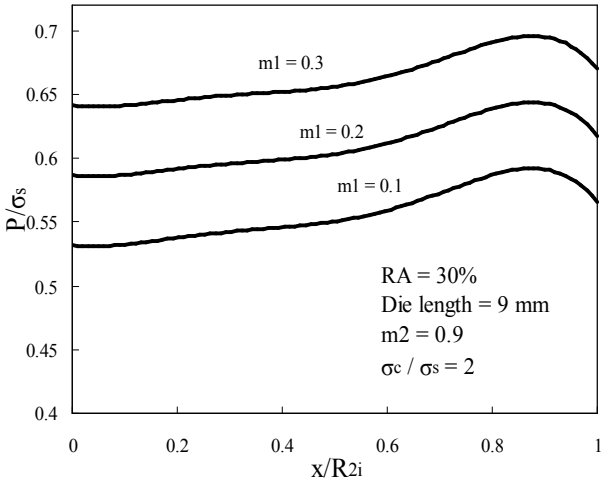


Figure 6. Effect of the friction factor between sleeve and die wall $m_1$ on the mode of deformation.

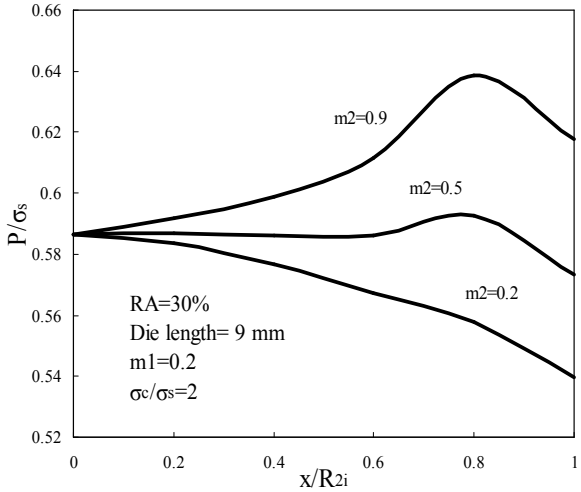

Figure 7. Effect of the friction factor between sleeve and core $m_2$ on the mode of deformation.

The effect of die length on the deformation mode for different values of friction factor is shown in Fig. 8.As it is expected, for a given value of friction factor, the relative extrusion pressure is minimized in an optimum die length. It is observed that the deformation mode is changed when shearing friction factor increases. From this figure, it is also seen that an increase in the friction factor tends to increase the relative extrusion pressure.

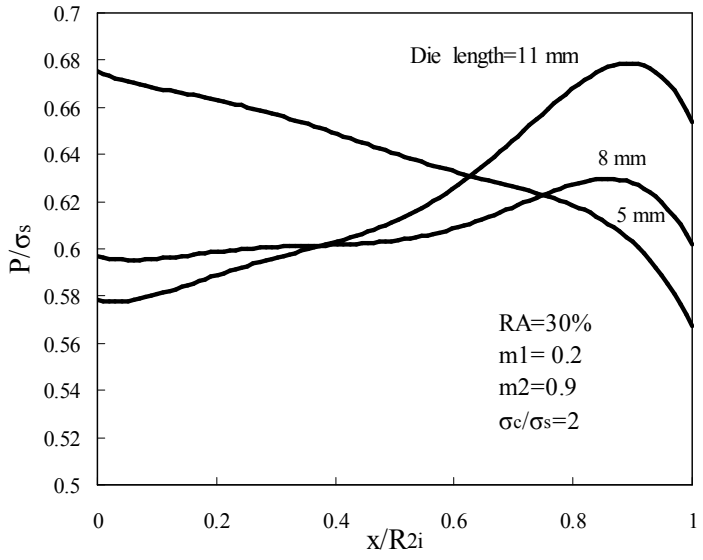


Figure 8. Effect of die length on the mode of deformation.

Fig. 9 shows the effect of reduction in area on the mode of deformation. As shown in this figure, the effect of friction on the mode of deformation is not marked, although the effect is great on the extrusion pressure

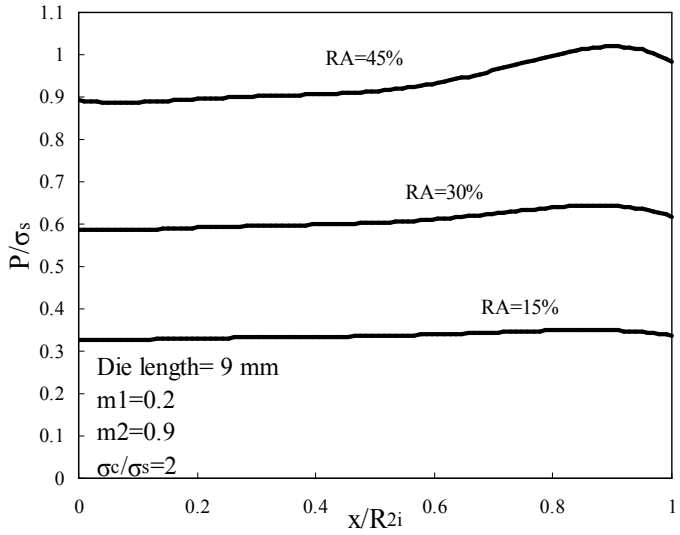


Figure 9. Effect of reduction in area on the mode of deformation.

## 5. CONCLUSIONS

In this research, a theoretical analysis of the modes of deformation of bi-metallic rod extrusion through dies of anyshape has been developed by using the upper bound method and the following results were extracted:

(1) Extrusion of a bi-metallic rod through arbitrarily curved die was analyzed at several yield stress ratios, and it has been found that uniform deformation occurs at low yield stress ratios.

(2) It was predicted that uniform deformation will be occurred when the frictional stress at the interface is high. The cladding type of deformation will occur when the inner material is hard, the interface friction is relatively low and the die length is large.

(3) The frictional shear factor of die surface and extrusion ratio do not effect on the mode of

deformation, although the effects are great on the relative extrusion pressure.
(4) The developed upper bound solution can be very beneficial in studying the influence of multiple variables and any dies hape on the deformation modes such as uniform deformation and cladding of bi-metallic rod extrusion process.

**Nomenclature**

$m_1$ :friction factor between sleeve and die

$m_2$ :friction factor between core and sleeve

$P$ : extrusion pressure

$r$ , $\theta$ , $\phi$ : spherical coordinates

$r_f$ , $r_{1f}$ , $r_{2f}$ :spherical radii of exit velocity discontinuity surfaces

$r_i$ , $r_{1i}$ , $r_{2i}$ :spherical radii of entrance velocity discontinuity surfaces

$R_{1f}$ :outer radius of sleeve at exit

$R_{2f}$ :outer radius of core in extruded bi-metallic rod

$R_{1i}$ :radius of container

$R_{2i}$ :outer radius of core in initial bi-metallic rod

$\Delta v$ :amount of velocity discontinuity

$L$ : length of die

$S$ :area of frictional or velocity discontinuity surface

$U_r$ , $U_\theta$ , $U_\phi$ :velocity components in spherical coordinate

$U_f$ , $U_{1f}$ , $U_{2f}$ : exit velocities

$U_i$ :entrance velocity

$J^*$ :externally supplied power of deformation

$\dot{W}_f$ :power dissipated on the frictional surfaces

$\dot{W}_i$ :internal power of deformation

$\dot{W}_S$ :power dissipated on the velocity discontinuity surfaces

$x$ :distance of origin $O_2$ from the axis of symmetry

*Greek symbols*

$\dot{\varepsilon}_{rr}$ , $\dot{\varepsilon}_{\theta\theta}$ , $\dot{\varepsilon}_{\phi\phi}$ :normal strain rate components in the radial, angular and rotational directions

$\dot{\varepsilon}_{r\theta}$ , $\dot{\varepsilon}_{r\phi}$ , $\dot{\varepsilon}_{\theta\phi}$ :shear strain rate components

$\eta$ :local angle of the die surface with respect to the local radial velocity component

$\eta_i$ :local angle of the interface surface with respect to the local radial velocity component

$\alpha$ :angle of the line connecting the initial point of the die to the final point of the die

$\beta$ :angle of the line connecting the initial point of the interface to the final point of the interface

$\gamma$ :arbitrary angle on the surface $S_2$

$\psi(r)$ :angular position of the die as a function of radial position

$\psi_i(r)$ , $\psi_{1i}(r)$ , $\psi_{2i}(r)$ :angular positions of the interface as a function of radial position from origins $O$ , $O_1$ and $O_2$, respectively

$\sigma_c$ :flow stress of the corematerial

$\sigma_s$ :flow stress of the sleevematerial

**REFERENCES**

[1] Osakada K., Limb M., Mellor P.B., "Hydrostatic extrusion of composite rods with hard cores", ***International Journal of Mechanical Sciences*** 15 291-307(1973).

[2] Ahmed N., "Extrusion of copper clad aluminum wire", ***Journal of Mechanical Working Technology***, 2:19–32(1978).

[3] Avitzur B. Handbook of Metal-Forming Processes, New York: ***Wiley,***(1983).

[4] Tokuno H., Ikeda K., "Analysis of deformation in extrusion of composite rods", ***Journal of Materials Processing Technology***26:323-335(1991).

[5] Yang D.Y., Kim Y.G., Lee C.M., "An upper-bound solution for axisymetric extrusion of composite rods through curved dies", ***International Journal of Mechanical Sciences***31:565-575(1991).

[6] Sliwa R., "Plastic zones in the extrusion of metal composites", ***Journal of Materials Processing Technology***67:29-35(1997).

[7] Kazanowski P., Epler M.E., Misiolek W.Z., "Bi-metal rod extrusion-process and product optimization", ***Materials Science and Engineering A*** 369:170–180 (2004).

[8] Nowotynska I., Smykla A. "Influence of die geometric parameters on plastic flow of layer composites during extrusion process", ***Journal of Materials Processing Technology***209 1943-1949(2009).

[9] Chitkara N.R.,Aleem A., "Extrusion of axi-symmetricbi-metallictubes: someexperimentsusinghollowbilletsandtheapplicatio n of a generalizedslabmethod of analysis", ***International Journal of MechanicalSciences*** 43 2857–2882(2001).

[10] Chitkara N.R.,Aleem A., "Extrusion of axi-symmetricbi-metallictubesfromsolidcircularbillets: application of a generalizedupper-boundanalysisandsomeexperiments", ***International Journal of MechanicalSciences***43:2833–2856(2001).

[11] Hwang Y.M., Hwang T.F., "An investigation into the plastic deformation behaviour within a conical die during composite rod extrusion"***, Journal of***

***Materials Processing Technology*** 121:226-233(2002).

[12] Khosravifard A., Ebrahimi R., "Investigation of parameters affecting interface strength in Al/Cu clad bimetal rod extrusion process", ***Materials and Design*** 31 493-499(2010).

[13] Gordon W.A., Van Tyne C.J., Moon Y.H., "Axisymmetric extrusion through adaptable dies—part 1: flexible velocity fields and power terms", ***International Journal of Mechanical Sciences*** 49 86–95(2007).

[14] Yang D.Y., Han C.H., "A new formulation of generalized velocity field for axi-symmetric forward extrusion through arbitrarily curved dies, Transactions of the ASME", ***Journal of Engineering for Industry*** 109:161–168(1987).

[15] Gordon W.A., Van Tyne C.J., Moon Y.H., "Axisymmetric extrusion through adaptable dies—part 3: minimum pressure streamlined die shapes", ***International Journal of Mechanical Sciences*** 49 104-115(2007).